Kinematic analysis of Active Ankle using computational algebraic geometry

Shivesh Kumar[1a], Abhilash Nayak[2], Bertold Bongardt[1a], Andreas Mueller[3] and Frank Kirchner[1ab]

[1a]*Robotics Innovation Center, German Research Center for Artificial Intelligence (DFKI GmbH), Bremen 28359, Germany e-mail: shivesh.kumar@dfki.de, bertold.bongardt@dfki.de*
[1b]*Universität Bremen, Fachbereich Mathematik und Informatik, Arbeitsgruppe Robotik, Bremen 28359, Germany e-mail: frank.kirchner@dfki.de*
[2]*IRCCyN, Ecole Centrale de Nantes, Nantes 44321, France, e-mail: Abhilash.Nayak@irccyn.ec-nantes.fr*
[3]*Institute of Robotics, Johannes Kepler University Linz, Linz 4040, Austria e-mail: a.mueller@jku.at*

Abstract. ACTIVE ANKLE is a novel 3 DoF parallel mechanism which works in an almost spherical manner. Its geometry provides various advantages like good stress distribution, low link diversity and robust construction. Determining all the solutions to the direct kinematics problem is an important and challenging step in kinematic analysis of any newly invented parallel manipulator due to the coupled nature of the constraint equations. In this paper, we make use of powerful methods in computational algebraic geometry to provide a rational univariate representation of direct kinematics solution in the form of a 40 degree univariate polynomial. In the presented analysis, up to 16 real solutions of the direct kinematics problem for this mechanism have been obtained. In addition, the results of its torsional motion analysis are presented and singularities of the mechanism are highlighted during this motion. Also, the assembly modes where this mechanism behaves as an almost-spherical device are identified, which is the main contribution of the paper.

Key words: parallel manipulator, kinematic analysis, direct kinematics, algebraic geometry.

1 Introduction

A novel, almost-spherical parallel manipulator (ASPM) ACTIVE ANKLE (Fig. 1) and its comparison with similar mechanisms like AGILE EYE has recently been introduced in [5] and [6]. Due to its unique, simple and compact $3[R2[SS]]$ design (topological equivalent of DELTA robot), the constraint of moving the end-effector about an exact center (of rotation) in case of spherical parallel manipulators (SPM) is relaxed to almost spherical motions that includes a shift of the end effector about a tolerated, very small domain. Due to the presence of a closed loop in each leg, the mechanism offers high stiffness and orientation accuracy. The mechanism features a low link diversity and its simple, robust and modular design makes it highly suitable for many applications. While the primary application of the ACTIVE ANKLE is an active ankle joint in an exoskeleton or a humanoid, it could also be integrated as a submechanism into a regional manipulator for obtaining precise six DOF motions

1

if the constrained translations of the ASPM are compensated by the previous joints of the overall device.

Solving the direct kinematics of any newly invented parallel manipulator is usually challenging. Since the last few decades, increasingly sophisticated computational tools are being developed for numerical algebraic geometry that can assist derivation and solution of polynomial systems which describe the mechanism geometry [2, 1]. This paper aims to provide the solution to direct kinematics problem (DKP) of the ACTIVE ANKLE mechanism using powerful tools from computational algebraic geometry. The motivation stems from the desire to identify those DKP solutions, i.e. the assembly modes, that have the lowest deviation from a perfect spherical motion. In particular, we are interested in exploring the upper bounds on the number of solutions of its DKP and identifying assembly modes where the mechanism behaves in an *almost-spherical* manner. The torsional motion of this mechanism corresponds to adduction-abduction movements when employed as an ankle joint (see [6] for foot interface unit) and hence analysis of this movement is of practical interest.

The paper is organized as follows: Section 2 presents the manipulator's architecture and constraint equations. Section 3 presents the solution to the direct kinematics problem by first deriving an upper bound on the total number of solutions and later exploring the number of real solutions by discretizing the configuration space. Section 4 presents the torsional motion analysis of this mechanism and highlights some of the singularities. Section 5 concludes the paper by summarizing new insights into the mechanism's geometry.
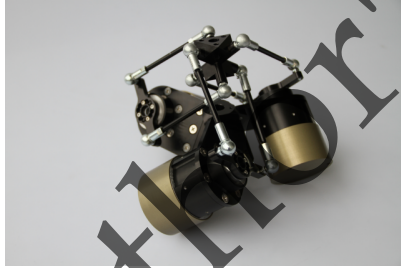
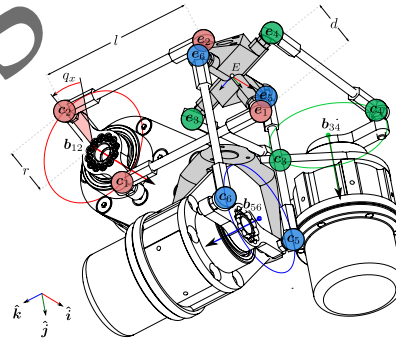

Fig. 1: ACTIVE ANKLE prototype

Fig. 2: ASPM architecture

2 Architecture and Constraint Equations

The mechanism ACTIVE ANKLE shown in Figure 2 comprises of three legs each of which consist of a revolute joint and a spatial quadrilateral linkage with four spherical joints. The motors actuate the three revolute joints whose axes are aligned

along the vectors $\hat{\mathbf{i}}$, $\hat{\mathbf{j}}$ and $\hat{\mathbf{k}}$. The fixed global coordinate frame G is chosen such that it is coincident with moving end effector coordinate frame E when the mechanism is in its zero configuration. The position vectors of the spherical joint centers are $\mathbf{c}_i$ (on the crank) and $\mathbf{e}_i$ (on the end-effector), $i = 1, 2, ..., 6$. The vector $\mathbf{e} = (e_x, e_y, e_z)^T$ indicates the position of the moving coordinate frame E. The connecting rod length, l, crank radius, r and half-length of end effector segment d $(= ||\mathbf{e} - \mathbf{e}_i||)$ constitute the design parameters. For input joint variables q_x, q_y and q_z, the homogeneous coordinates of $\mathbf{c}_i$ in the ground frame G and $\mathbf{e}_i$ in the end-effector frame E are written as follows:

$$
\begin{aligned}
\mathbf{c}_1^G &= [1, 0, r\cos(q_x), l + r\sin(q_x)]^T & \mathbf{e}_1^E &= [1, 0, d, 0]^T \\
\mathbf{c}_2^G &= [1, 0, -r\cos(q_x), l - r\sin(q_x)]^T & \mathbf{e}_2^E &= [1, 0, -d, 0]^T \\
\mathbf{c}_3^G &= [1, l + r\sin(q_y), 0, r\cos(q_y)]^T & \mathbf{e}_3^E &= [1, 0, 0, d]^T \\
\mathbf{c}_4^G &= [1, l - r\sin(q_y), 0, -r\cos(q_y)]^T & \mathbf{e}_4^E &= [1, 0, 0, -d]^T \\
\mathbf{c}_5^G &= [1, r\cos(q_z), l + r\sin(q_z), 0]^T & \mathbf{e}_5^E &= [1, d, 0, 0]^T \\
\mathbf{c}_6^G &= [1, -r\cos(q_z), l - r\sin(q_z), 0]^T & \mathbf{e}_6^E &= [1, -d, 0, 0]^T
\end{aligned}
\tag{1}
$$

To express $\mathbf{e}_i$ in the global frame, a coordinate transformation is used as follows:

$$
\mathbf{e}_i^G = \mathbf{M}\,\mathbf{e}_i^E
\tag{2}
$$

where, $\mathbf{M}$ is the transformation matrix algebraically described by unit quaternions and position coordinates. With this choice, we obtain a formulation in terms of 7 parameters which further eases the Gröbner basis computation.

$$
\mathbf{M} = \begin{bmatrix}
1 & 0 & 0 & 0 \\
e_x & x_0^2 + x_1^2 - x_2^2 - x_3^2 & -2x_0x_3 + 2x_1x_2 & 2x_0x_2 + 2x_1x_3 \\
e_y & 2x_0x_3 + 2x_1x_2 & x_0^2 - x_1^2 + x_2^2 - x_3^2 & -2x_0x_1 + 2x_3x_2 \\
e_z & -2x_0x_2 + 2x_1x_3 & 2x_0x_1 + 2x_3x_2 & x_0^2 - x_1^2 - x_2^2 + x_3^2
\end{bmatrix}
\tag{3}
$$

where, e_x, e_y and e_z represent the position of the end effector center in the global frame. The parameters x_i $(i = 0, ..., 3)$ are the orientation quaternions satisfying:

$$
g_1 := x_0^2 + x_1^2 + x_2^2 + x_3^2 - 1 = 0
\tag{4}
$$

The distance between $\mathbf{c}_i$ and $\mathbf{e}_i$ is fixed and equal to rod length l (see Fig. 2). Thus, we can set up six constraint equations for this mechanism:

$$
||\mathbf{e}_i - \mathbf{c}_i||^2 = l^2 \quad i = 1, ..., 6
\tag{5}
$$

The six constraint equations after simplifications along with orientation quaternion normalization equation ($g_1 = 0$) form an ideal $\mathfrak{I} = \langle g_1, g_2, g_3, g_4, g_5, g_6, g_7 \rangle$, where:

$$g_2 := (-4e_z r + 4lr)\sin q_x - 4r\cos q_x e_y - 8e_x d(x_0 x_3 - x_1 x_2)$$
$$+ 4e_y d(x_0^2 - x_1^2 + x_2^2 - x_3^2) + 8e_z d(x_0 x_1 + x_2 x_3) - 8dl(x_0 x_1 + x_2 x_3) = 0 \quad (6)$$

$$g_3 := (-4e_y r + 4lr)\sin(q_z) - 4r\cos(q_z)e_x - 8e_z d(x_0 x_2 - x_1 x_3)$$
$$+ 4e_x d(x_0^2 + x_1^2 - x_2^2 - x_3^2) + 8e_y d(x_0 x_3 + x_1 x_2) - 8dl(x_0 x_3 + x_1 x_2) = 0 \quad (7)$$

$$g_4 := (-4e_x r + 4lr)\sin(q_y) - 4r\cos(q_y)e_z - 8e_y d(x_0 x_1 - x_2 x_3)$$
$$+ 4e_z d(x_0^2 - x_1^2 - x_2^2 + x_3^2) + 8e_x d(x_0 x_2 + x_1 x_3) - 8dl(x_0 x_2 - x_1 x_3) = 0 \quad (8)$$

$$g_5 := (-8drx_0 x_1 - 8drx_2 x_3)\sin(q_x) + 2e_x^2 + 2e_y^2 + 2e_z^2 - 4e_z l + 2d^2 + 2r^2$$
$$+ (-4drx_0^2 + 4drx_1^2 - 4drx_2^2 + 4drx_3^2)\cos(q_x) = 0 \quad (9)$$

$$g_6 := (-8drx_0 x_3 - 8drx_1 x_2)\sin(q_z) + 2e_x^2 + 2e_y^2 + 2e_z^2 - 4e_y l + 2d^2 + 2r^2$$
$$+ (-4drx_0^2 - 4drx_1^2 + 4drx_2^2 + 4drx_3^2)\cos(q_z) = 0 \quad (10)$$

$$g_7 := (-8drx_0 x_2 - 8drx_1 x_3)\sin(q_y) + 2e_x^2 + 2e_y^2 + 2e_z^2 - 4e_x l + 2d^2 + 2r^2$$
$$+ (-4drx_0^2 + 4drx_1^2 + 4drx_2^2 - 4drx_3^2)\cos(q_y) = 0 \quad (11)$$

3 Solving Direct Kinematics

The sine and cosine in Eq. (6) to (11) are replaced with the tangent half-angle expressions: $\sin(q_i) = \frac{2t_i}{1+t_i^2}$ $\cos(q_i) = \frac{1-t_i^2}{1+t_i^2}$ where, $t_i = \tan(\frac{q_i}{2})$, $i = x, y, z$. To this end, t_x, t_y and t_z are the inputs and $x_0, x_1, x_2, x_3, e_x, e_y$ and e_z are the outputs to be solved for in the seven equations $g_i = 0$, $i = 1..7$. The design parameters are substituted as $l = 10$ cm, $d = r = 3.5$ cm.

3.1 Rational Univariate Representation of DKP Solution

A Gröbner basis of the ideal $\mathfrak{I} = \langle g_1, g_2, g_3, g_4, g_5, g_6, g_7 \rangle$ is calculated over the field $\mathbb{K}[x_0, x_1, x_2, x_3, e_x, e_y, e_z]$. It was possible to compute the Gröbner basis only after substituting certain values to the inputs q_x, q_y and q_z and to the design parameters. For the lexicographic ordering $x_0 <_{lex} \{e_j, x_i\}$ and $x_i <_{lex} \{e_j, x_0\}$ ($i = 1, 2, 3; j = x, y, z$), the univariate polynomial in x_0 and x_i turned out to be of degree 28 and 75, respectively which should be halved to find unique solutions due to Eq. (4). For $e_j <_{lex} x_i$ ($i = 0, 1, 2, 3; j = x, y, z$), the polynomial in e_j was of degree 40. Hence, a bound on the maximum number of solutions can be found as $\max\{28/2, 75/2, 40\}$. Thus, the ACTIVE ANKLE can have a maximum of 40 direct kinematic solutions.

3.2 Finding Real Solutions

For $t_x = t_y = t_z = \tan(\frac{30^\circ}{2})$, the **RootFinding[Isolate]** function of Maple is used to find out all the real solutions for the set of constraint equations. The algorithm

No.	e_x (cm)	e_y (cm)	e_z (cm)	a_x	a_y	a_z	θ (deg)
1	1.69	1.69	1.69	-0.57	-0.57	-0.57	159.1°
2	4.93	4.93	4.93	-0.57	-0.57	-0.57	148.7°
3	0.06	0.06	0.06	-0.57	-0.57	-0.57	44.3°
4	6.6	6.6	6.6	-0.57	-0.57	-0.57	23.6°
5	0.69	2.12	2.59	-0.28	0.12	-0.94	139.4°
6	2.12	2.59	0.69	0.12	-0.94	-0.28	139.4°
7	2.6	0.69	2.12	0.94	0.28	-0.12	139.4°
8	1.82	3.47	3.78	-0.16	0.32	-0.93	157°
9	3.78	1.82	3.47	0.93	0.16	-0.32	157°
10	3.47	3.78	1.82	0.32	-0.93	-0.16	157°
11	0.63	0.89	1.43	-0.57	0.22	-0.78	107.3°
12	0.89	1.43	0.63	0.22	-0.78	-0.57	107.3°
13	1.43	0.63	0.89	0.78	0.57	-0.22	107.3°
14	5.16	5.88	5.37	0.52	0.06	-0.84	86.1°
15	5.88	5.37	5.16	-0.06	0.84	-0.52	86.1°
16	5.37	5.16	5.88	0.84	-0.52	-0.06	86.1°

Table 1: Overview of 16 solutions for the DKP with $q_x = q_y = q_z = 30°$.

behind this function finds out the rational univariate representation of the set of polynomials and isolates the real roots of these univariate polynomials based on Descartes' rule of sign and the bisection strategy in a unified framework [4].

A total of 32 direct kinematic solutions are obtained for $q_x = q_y = q_z = 30°$. Due to Eq. (4), this number is to be halved to discard repeated roots. Thus, there are 16 unique assembly modes for the given input. For each assembly mode, the end effector position (e_x, e_y, e_z) and the axis-angle representation (a_x, a_y, a_z, θ) are expressed as follows: $a_x = \frac{x_1}{\sqrt{1-x_0^2}}, \quad a_y = \frac{x_2}{\sqrt{1-x_0^2}}, \quad a_z = \frac{x_3}{\sqrt{1-x_0^2}}, \quad \theta = 2\cos^{-1}(x_0)$. The configuration of these assembly modes is listed in Table 1.

Among them, No. 3 and 4 are shown in Figures 3 and 4. The points corresponding to the position vector $\mathbf{c}_i$ can move on the circumference of those circles drawn. The points $\mathbf{e}_i$ form a spatial cross, the center of which represents the end effector point (shown as black sphere). No. 1 − 4 show the assembly modes where $e_x = e_y = e_z$ and $a_x = a_y = a_z$. Since, $q_x = q_y = q_z$, the other twelve assembly modes are observed in triplets with the same axis angle θ and permuted values of (e_x, e_y, e_z) and (a_x, a_y, a_z). Four such triplets are observed in solutions 5 to 7, 8 to 10, 11 to 13 and 14 to 16 in Table 1. This pattern may not be visible when $t_i \neq t_j \ \forall i, j = x, y, z$. In addition, this method is used to record the percentage of number of real solutions to DKP by varying q_x, q_y and q_z from $-180°$ to $180°$ in finite increments [3]. For convenience, the configuration space is partitioned into 1331 permutations of input angles and the results are shown in Table 2. It may be noted that the number of real solutions for any configuration can only be an even number due to an even upper bound on the total number of solutions.
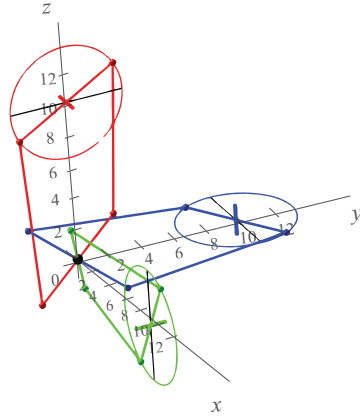
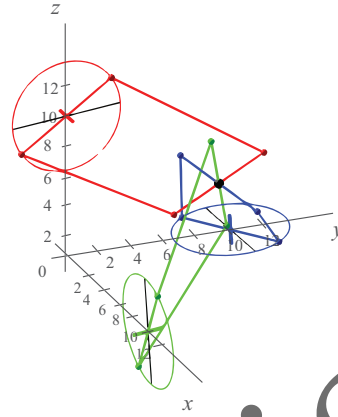Fig. 3: Assembly Mode 3 (refer Table 1)   Fig. 4: Assembly Mode 4 (refer Table 1)

Real solutions	0	2	4	6	8	10	12	14	16	Σ
Complex solutions	40	38	36	34	32	30	28	26	24	
Number of poses	204	282	237	222	287	83	12	0	4	1331
Fraction of poses	15.33	21.19	17.80	16.68	21.56	6.24	0.90	0	0.30	100%

Table 2: Overview of the solvability of the DKP for $q = (q_x, q_y, q_z)^T \in \mathsf{S}^3$ with discretization $\mathsf{S} = [-180°, 180°]$ in 11 steps ($|\mathsf{S}| = 11$ and $|\mathsf{S}^3| = 1331$).

4 Torsional Motion Analysis

The torsional motion of this manipulator is of practical interest because it corresponds to the adduction-abduction movement when employed as an ankle joint. The torsional motion can be characterized by substituting $e_x = e_y = e_z = e$ and $t_x = t_y = t_z = t$ in seven constraint equations. The Gröbner basis for the ideal $\Im$, now defined over a reduced field $\mathbb{K}[x_0, x_1, x_2, x_3, e]$, is calculated with pure lexicographic order $e <_{lex} x_3 <_{lex} x_2 <_{lex} x_1 <_{lex} x_0$ using Maple software. This yields a Gröbner basis consisting of five polynomials, out of which the first one is an input (t) – output (e) agnostic description of the mechanism.

$$
\begin{aligned}
G_1 := & (9t^8 + 36t^6 + 54t^4 + 36t^2 + 9)e^4 + (-1347t^8 - 441t^7 - 4359t^6 - 1029t^5 \\
& - 5877t^4 - 735t^3 - 4065t^2 - 147t - 1200)e^3 + (74251t^8 + 14700t^7 \\
& + 142899t^6 + 44296t^5 + 139207t^4 + 54096t^3 + 98701t^2 + 24500t + 47350)e^2 \\
& + (-1710100t^8 + 980000t^7 + 220500t^6 + 19600t^5 + 1239700t^4 - 19600t^3 \\
& + 739900t^2 - 980000t - 490000)e + 12005000t^8 - 24010000t^7 - 12005000t^6 \\
& + 48020000t^5 - 12005000t^4 - 24010000t^3 + 12005000t^2 = 0
\end{aligned}
$$

$$(12)$$

It shows that a maximum of four assembly modes and a maximum of eight working modes (solutions to the inverse kinematics problem) are possible on the subvariety defined by $e_x = e_y = e_z$. The implicit plot of Eq. (12) after substituting $t = \tan(q/2)$ is shown in Figure 5 for $e = 0, ..., 7$cm and $q = q_x = q_y = q_z = -180°, ..., 180°$. For a value of $q = q_x = q_y = q_z = 30°$, four values of e observed in this figure match with the values noted in Table 1. From Figure 5, one could also note that the assembly modes shown in Figures 3 and 4 were actually the *almost-spherical* assembly modes for this mechanism because in these assembly modes the change in end effector's position is minimal.

The second equation of Gröbner's basis in e, t and x_0 is found out to be:

$$G_2 := \left(9t^4 + 18t^2 + 9\right)e^2 + \left(-600t^4 - 294t^3 - 906t^2 - 600\right)e$$
$$+ \left(9800t^4 - 9800\right)x_0{}^2 + 4900t^4 - 14700t^2 + 9800 = 0 \tag{13}$$

Eliminating e from Eq. (12) and (13) and substituting $t = \tan(q/2)$ and $x_0 = \cos(\theta/2)$ results in an implicit equation in terms of the axis angle θ (representing the rotational workspace) and the actuated variable q. Figure 6 shows the implicit plot of q vs. θ for $\theta = -180°, ..., 180°$ and $q = q_x = q_y = q_z = -180°, ..., 180°$.
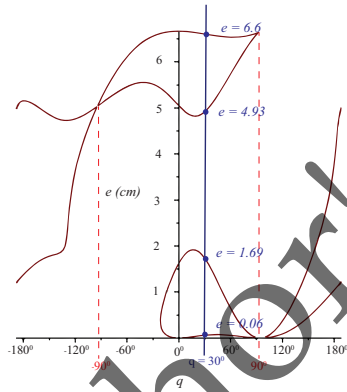

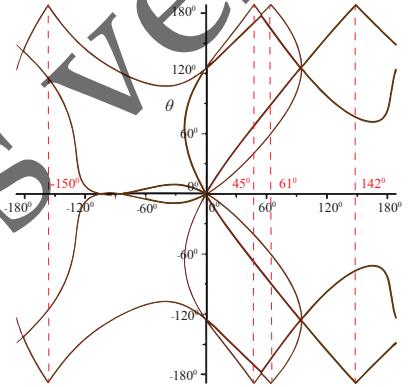Fig. 5: Implicit plot between q and e Fig. 6: Implicit plot between q and θ

A Jacobian matrix $\mathbf{J}$ of dimension 5×5 is calculated by partially differentiating the constraint polynomials with respect to the variables of the considered field. When the determinant of this Jacobian vanishes, the mechanism reaches a singularity. Considering the Gröbner basis equations and $det(\mathbf{J}) = 0$, other variables are eliminated to obtain the Eq. (14) only in terms of $t_x = t_y = t_z = t = \tan(q/2)$.

$$det(\mathbf{J}) := (t-1)(t+1)(t^2+1)(2601t^{12} - 408t^{11} - 55370t^{10} + 54732t^9$$
$$+ 240101t^8 - 491700t^7 + 771464t^6 - 925624t^5 + 751804t^4 \tag{14}$$
$$- 497200t^3 + 259600t^2 - 80000t + 10000) = 0$$

Solving for t and hence q results in six unique solutions which are noticeable as cusps in Figures 5 and 6. For instance, $q = 90°$ is one of the singularities when e reaches a value of 6.6 cm. Since, other values of e are indeed possible for an input angle of $90°$, it is important to mention the magnitude of the pair $\{e,q\}$ or $\{\theta,q\}$ while representing these singularities.

5 Conclusion

This paper presents some global insights into the geometry of the ACTIVE ANKLE mechanism through its direct kinematics analysis using tools from computational algebraic geometry. It is established that the upper bound to the number of unique solutions to direct kinematics problem is 40 which supports our observation that once the actuator angles are fixed in the three legs, ACTIVE ANKLE behaves as a special instance of $6 - 6$ STEWART platform. In practice, a maximum of 16 real solutions of the direct kinematics problem were found. In addition, the results of the torsional motion analysis which is of practical interest is presented and some singularities of the mechanism are highlighted. Moreover, the assembly modes where the mechanism behaves as an *almost-spherical* device are identified.

References

[1] Husty, M.L., Pfurner, M., Schröcker, H.P., Brunnthaler, K.: Algebraic methods in mechanism analysis and synthesis. Robotica **25**(6), 661–675 (2007)
[2] McCarthy, J.M. (ed.): 21st Century Kinematics. Springer-Verlag London (2013)
[3] Merlet, J.: Parallel Robots, chap. Direct kinematics, pp. 105–152. Springer Netherlands, Dordrecht (2006)
[4] Rouillier, F.: Efficient isolation of polynomial's real roots. Journal of Computational and Applied Mathematics **162**(1), 33 – 50 (2004)
[5] Simnofske, M.: Ausrichtungsvorrichtung zum Ausrichten einer Plattform in drei rotatorischen Freiheiten. Patent application, DE102013018034A1 (2015)
[6] Simnofske, M., Kumar, S., Bongardt, B., Kirchner, F.: Active ankle - an almost-spherical parallel mechanism. In: 47th International Symposium on Robotics (ISR), June 21-22, Munich, Germany. VDE Verlag (2016)